

See discussions, stats, and author profiles for this publication at: <https://www.researchgate.net/publication/265251740>

Numerical Study of an Oscillating Wave Energy Converter with Nonlinear Snap-Through Power-Take-Off Systems in...

Conference Paper · June 2014

DOI: 10.13140/2.1.4414.4000

CITATIONS

2

READS

117

3 authors, including:



Xiantao Zhang

University of Western Australia

14 PUBLICATIONS 12 CITATIONS

SEE PROFILE

Some of the authors of this publication are also working on these related projects:



Green water for ship-type offshore structures [View project](#)



Application of bistable potential (negative stiffness) mechanism to oscillating-body wave energy converters [View project](#)

Numerical Study of an Oscillating Wave Energy Converter with Nonlinear Snap-Through Power-Take-Off Systems in Regular Waves

Xiantao Zhang, Jianmin Yang, Longfei Xiao

State Key Laboratory of Ocean Engineering, Shanghai Jiao Tong University
 Shanghai, China

ABSTRACT

In this paper, a nonlinear snap-through Power-Take-Off system is applied to a hemispherical wave energy converter oscillating in heave direction in regular waves. The nonlinear Power-Take-Off system is consisted of two symmetrically oblique springs and a linear damper, which is characteristic of negative stiffness and double-well potential. The dynamic response of the converter with nonlinear Power-Take-Off system is numerically calculated using 4th order Runge-Kutta method. Results shows that the nonlinear snap through mechanism, compared with linear mechanism, can enhance power capture of the converter, especially in low frequency regular waves.

KEY WORDS: Wave energy; Power-Take-Off; snap through; linear; dynamic response

INTRODUCTION

Among various types of wave energy converters, the oscillating body (or point absorber) is rather promising, especially for deployment in offshore regions (Falcao, 2010). The oscillating motion of a floating body is converted to electricity by the Power-Take-Off (PTO) system of the wave energy converter. Usually the PTO system is simplified as a linear spring and a linear damper. Thus frequency domain analysis is used due to its simplicity and low computer requirement (Gomes et al. 2012). Falnes (2002) pointed out that for a single degree-of-freedom point absorber, the maximum power can be obtained at the resonance state in which the frequency of incident regular waves equals the natural frequency of the converter. However, the conversion is less powerful with wave periods off resonance, in particular so if the resonance bandwidth is narrow.

Thus it motivates us to make use of nonlinear mechanism in the PTO system to enhance power capture. Nonlinear mechanism including snap through is first studied in the realm of vibration energy instead of wave energy utilization. The snap through vibrations have been recognized as a means by which to dramatically improve energy harvesting performance for vibration energy harvesters (Tang et al. 2010; Stanton et al. 2010). Harne and Wang (2013) made a review of the snap through mechanism applied in vibration energy harvesting. They presented a common framework for snap through electromechanical dynamics and

also listed some remaining challenges. Ramlan et al. (2010) analyzed the dynamic response of a snap through mechanism consisting of two symmetrically spring and a damper. The response of the snap through vibration system is either chaotic or periodic for different input level.

In what follows, a nonlinear snap through PTO system, which consists of a linear damper and two symmetrically springs, is applied to a hemispherical wave energy converter oscillating in heave direction in regular waves. First, the static characteristic of the snap through mechanism is analyzed in a detailed way. Then the dynamic response of the converter with linear and nonlinear snap through mechanism is numerically calculated using 4th order Runge-Kutta method. Comparisons of power capture are made between nonlinear and linear converters. And the effects of different parameters on the power capture are discussed.

THE MODEL

A floating hemisphere is chosen as the geometry of the converter. The hemisphere is rigidly connected to the PTO system. The hemisphere is restricted to only heave oscillation. And the water depth is supposed to be infinite. Fig.1 is the hemispherical converter with nonlinear snap through PTO mechanism. And Fig.2 is the converter with linear PTO mechanism.

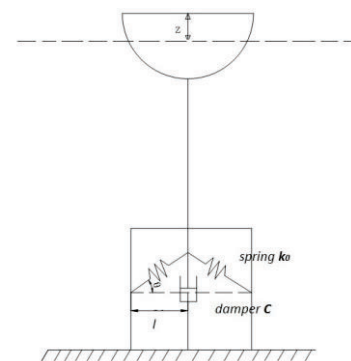


Fig.1 A hemispherical converter with nonlinear PTO system

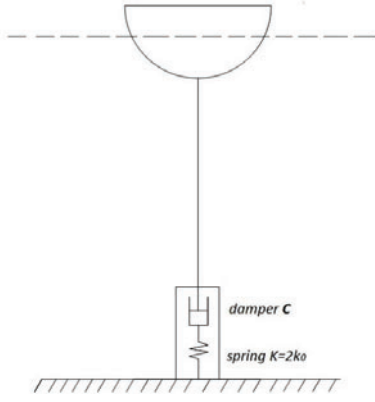


Fig.2 A hemispherical converter with linear PTO system

STATIC CHARACTERISTIC OF SNAP THROUGH MECHANISM

The arrangement of two oblique springs for snap through mechanism is shown in Fig.3.

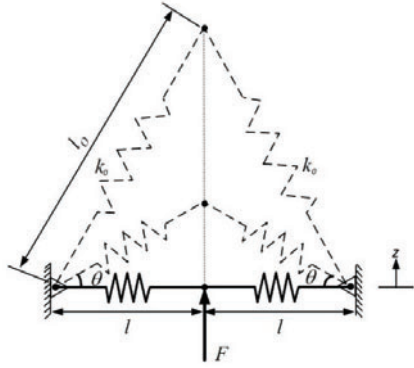


Fig.3 The arrangement of springs for snap through mechanism

Suppose the vertical force F is applied to keep equilibrium of the snap through spring system. z is the vertical direction.

$$F = 2k_0(\sqrt{z^2 + l^2} - l_0) \frac{z}{\sqrt{z^2 + l^2}} \quad (1)$$

$$= 2k_0(1 - \frac{l_0}{\sqrt{z^2 + l^2}})z$$

where, l is half of the horizontal distance between the two springs, l_0 is the original length of both springs without extension and compression and k_0 is the stiffness of the spring. Eq. (1) can be expressed in the non-dimensional form as

$$F^* = (1 - \frac{1}{\sqrt{z^{*2} + \gamma^2}})z^* \quad (2)$$

with $F^* = \frac{F}{2k_0 l_0}$, $z^* = \frac{z}{l_0}$, $\gamma = \frac{l}{l_0}$.

Fig.4 shows F^* as a function of z^* for various values of γ . It can be seen that a negative stiffness arises up for $0 < \gamma < 1$. The smaller value of γ , the more negative of stiffness.

The potential energy can be expressed as follows,

$$E_p = 2[\frac{1}{2}k_0(\sqrt{z^2 + l^2} - l_0)^2] \quad (3)$$

Dimensionless form can be written as

$$E_p^* = (\sqrt{z^{*2} + \gamma^2} - 1)^2 \quad (4)$$

with $E_p^* = E_p / k_0 l_0^2$. E_p^* as a function of z^* is shown in Fig.5. Obviously, the snap through system is characteristic of double-well potential. And the motion response of the system may be local near one stable equilibrium position or overall across the potential barrier.

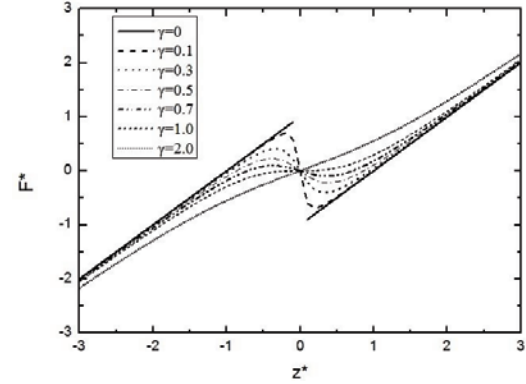


Fig.4 F^* as a function of z^* for various values of γ

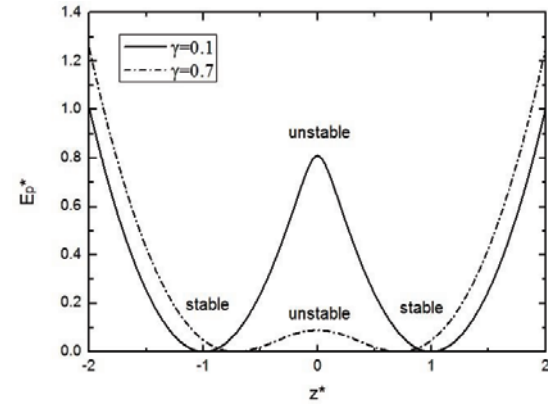


Fig.5 The dimensionless energy E_p^* as a function of z^*

THEORY OF DYNAMIC RESPONSE IN REGULAR WAVES

For regular waves of a given angular frequency ω , the governing equation for heave oscillation of the hemispherical converter with nonlinear snap through PTO system is, as indicated by Faltisen(1990), as follows,

$$(m + A_z)\ddot{z} + B_z\dot{z} + \rho g S z = f_d - C\dot{z} - K(1 - \frac{l_0}{\sqrt{l^2 + z^2}})z \quad (5)$$

And the governing equation for the converter with linear PTO system is

$$(m + A_z)\ddot{z} + B_z\dot{z} + \rho g S z = f_{dz} - C\dot{z} - Kz \quad (6)$$

here, z , \dot{z} and \ddot{z} are the displacement, velocity and acceleration for the heave oscillation, respectively. A_z and B_z are the hydrodynamic coefficients of added mass and radiation damping for heave oscillation. f_{dz} is the wave excitation forces consisting of Froude-Kriloff forces and diffraction forces due to the incident regular waves. C is the damping coefficient for both the nonlinear and linear PTO systems. K is the stiffness of the spring for the linear PTO system, while twice of the stiffness of each spring for the nonlinear PTO mechanism. This is convenient for the comparison of linear and nonlinear PTO system. ρ is the density of water. g is the acceleration of gravity. m is the mass of the hemispherical floater with values of $2\pi/3\rho a^3$. And a is the radius of the hemisphere. S is the area of the cross section of the hemisphere at the still water level and $S = \pi a^2$.

The moduli of the wave excitation force is proportional to the wave amplitude under linear assumption. And the proportionality for axisymmetric body (Falnes, 2002) is

$$\Gamma_z(\omega) = \frac{|f_{dz}|}{|A_\omega|} = \left(\frac{2g^3 \rho B_z}{\omega^3} \right)^{1/2} \quad (7)$$

here, A_ω is the wave amplitude and $|\cdot|$ denotes the moduli of a complex parameter.

Hulme(1982) gave the tabulated values, as well as asymptotic expressions, for the coefficients of added mass and radiation damping of a floating hemisphere oscillating in deep water in dimensionless form. And the physical parameters are related to the dimensionless ones as follows,

$$A_z = A^{(0)} \frac{2}{3} \pi \rho a^3 \quad (8)$$

$$B_z = B^{(0)} \frac{2}{3} \pi \rho a^3 \omega \quad (9)$$

with $A^{(0)}$ and $B^{(0)}$ being dimensionless coefficients of added mass and radiation damping respectively.

By defining $z^* = z/l_0$, $\dot{z}^* = \dot{z}/[l_0(g/a)^{1/2}]$, $\ddot{z}^* = \ddot{z}/[l_0(g/a)]$,

$$A_\omega^* = A_\omega/l_0, \quad \omega^* = \omega(a/g)^{1/2}, \quad K^* = K/\rho g S, \quad C^* = C\rho^{-1}a^{-5/2}g^{-1/2},$$

$$t^* = t(g/a)^{1/2}, \quad \gamma = l/l_0, \quad \dot{z}^* = dz^*/dt^*, \quad \ddot{z}^* = d^2z^*/dt^{*2}. \quad \text{Eq. (5) and Eq.6}$$

can be rewritten in non-dimensional form as

$$\ddot{z}^* + M\dot{z}^* + N[1 + K^*(1 - \frac{1}{\sqrt{\gamma^2 + z^{*2}}})]z^* = Q \cos \omega^* t^* \quad (10)$$

$$\ddot{z}^* + M\dot{z}^* + N(1 + K^*)z^* = Q \cos \omega^* t^* \quad (11)$$

together with

$$M = \frac{2}{3} \frac{\pi B^{(0)} \omega^* + C^*}{\pi(1 + A^{(0)})} \quad (12)$$

$$N = \frac{1}{\frac{2}{3} \pi(1 + A^{(0)})} \quad (13)$$

$$Q = \frac{2 \sqrt{\frac{\pi}{3}} \frac{\sqrt{B^{(0)}}}{\omega^*} A_\omega^*}{\frac{2}{3} \pi(1 + A^{(0)})} \quad (14)$$

Then the dynamic response of the hemispherical oscillating wave energy converter can be numerically calculated using 4th order Runge-Kutta method with the initial state of $z^* = 0$ and $\dot{z}^* = 0$. After the velocity of the converter is obtained, the power capture by the converter can be calculated using the expression as

$$P = \frac{1}{T} \int_0^T C \dot{z}^2 dt \quad (15)$$

Also the dimensionless form is as follows,

$$P^* = \frac{P}{\rho l_0^2 a^{1.5} g^{1.5}} = \frac{1}{T^*} \int_0^{T^*} C^* \dot{z}^{*2} dt^* \quad (16)$$

RESULTS

For the resonance condition, the non-dimensional circular frequency of the model in this paper is 1.08, and the dimensionless damping coefficient of PTO systems is about 0.49. In order to study the effects of different parameters on the absorbed power for both linear and nonlinear converters, different values of damping coefficient C^* , wave amplitude A_ω^* and nonlinear parameter γ are applied for calculation in the frequency domain. The value of dimensionless stiffness is chosen as $K^* = 0.1$, indicated by Vicente et al. (2013). The value of dimensionless circular frequency is chosen between 0 and 2 with the interval of 0.1. And for each frequency, the response is calculated for a time length of 100 periods. And only the last 50 periods are chosen for calculation of averaged power in order to omit the transient effects of initial state.

Figs.6 -8 are the numerical results of absorbed power by both linear and nonlinear converters for different incident wave amplitudes.

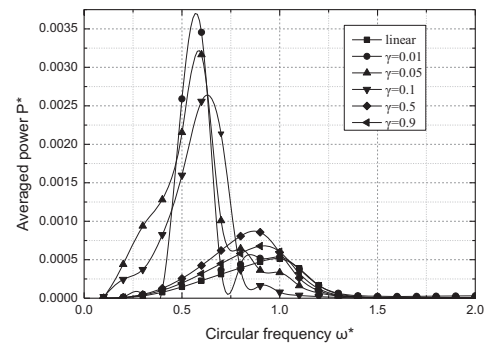


Fig.6 Absorbed power for linear and nonlinear converters with parameter $A_\omega^* = 0.1$, $C^* = 0.49$, $K^* = 0.1$

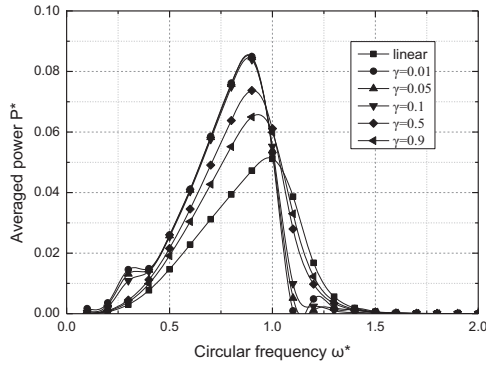


Fig.7 Absorbed power for linear and nonlinear converters with parameter $A_w^* = 1$, $C^* = 0.49$, $K^* = 0.1$

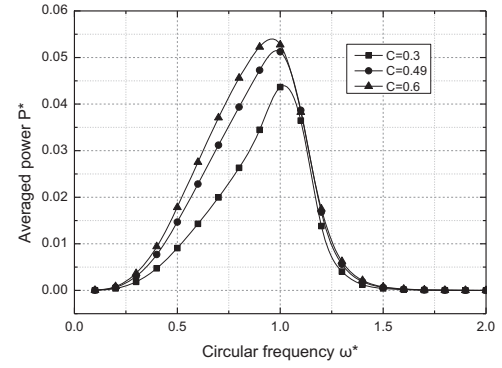


Fig.9 Averaged power by linear converters for different values of damping coefficient C^* together with $A_w^* = 1$, $K^* = 0.1$

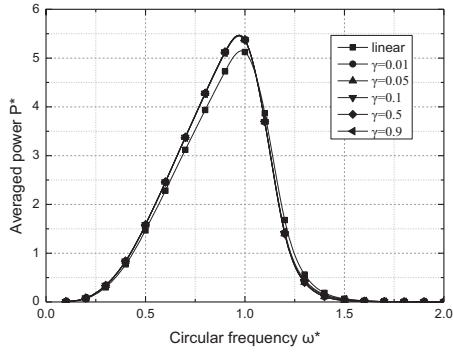


Fig.8 Absorbed power for linear and nonlinear converters with parameter $A_w^* = 10$, $C^* = 0.49$, $K^* = 0.1$

It can be seen that for small amplitude of regular waves, the averaged power absorbed by the nonlinear PTO systems is greatly larger than that by linear systems at relatively low frequency input. The smaller values of nonlinear parameter γ , the larger values of maximum power gained by nonlinear converters. However, the averaged power absorbed by nonlinear PTO system is less than that by linear systems when the input frequency is near resonance one. While in high input frequency condition, the difference of harvesting power between linear and nonlinear converters is small.

As the input wave amplitude increases (shown in Fig.7 and Fig.8), the difference of absorbed power between linear and nonlinear converters decreases despite of the facts that nonlinear converters still harvested more energy than linear ones at low frequency input.

Figs.9-11 are some numerical results of power capture by nonlinear and linear wave energy converters for different damping of PTO system. although $C^* = 0.49$ is the optimum damping coefficient at resonance frequency input, increase of values of C^* can lead to larger harvested power at lower or higher frequency than resonance one. Similar trends can be found for nonlinear converters with different nonlinear parameter γ .

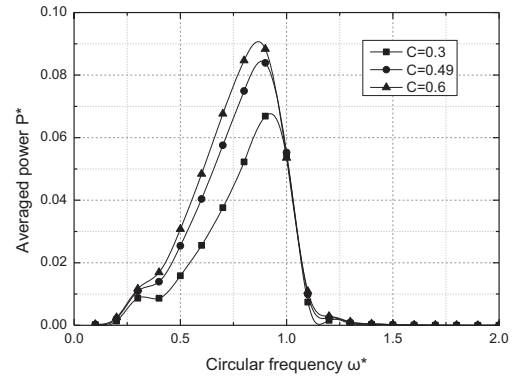


Fig.10 Averaged power by nonlinear converters for different values of damping coefficient C^* , together with $A_w^* = 1$, $K^* = 0.1$, $\gamma = 0.1$

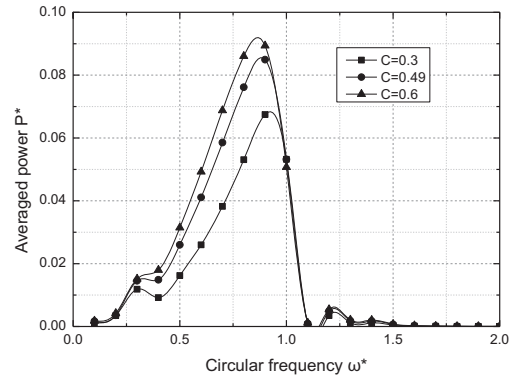


Fig.11 Averaged power by nonlinear converters for different values of damping coefficient C^* , together with $A_w^* = 1$, $K^* = 0.1$, $\gamma = 0.01$

Figs.12~13 are some illustrated examples of the steady state time history of the displacement and velocity response and the phase portrait for different parameters. It can be seen in Fig.12 that for nonlinear parameter $\gamma = 0.01$, the oscillating body just oscillates about a stable equilibrium position in a sinusoidal form at low frequency input as shown in Fig.12(a)~(b). However, the stable equilibrium position is opposite for $\omega^* = 0.1$ and $\omega^* = 0.3$. A further increase in the frequency introduces a cross-well motion which results in the response being

chaotic (Fig.12 (c)). As the frequency increases further, the cross-well motion vanishes as the body returns to oscillate about one of the stable equilibrium positions (Fig.12(d)~(e)).

For the nonlinear parameter $\gamma=0.1$, which can be seen from Fig.13, the oscillation of the wave energy converter is all cross-well for the five circular frequencies. At low frequency input (Fig.13(a)~(b)), the cross-well motion is chaotic. This may due to the fact that the input is small and the oscillating body could pass the potential barrier (the unstable equilibrium shown in Fig.5) occasionally. As the input frequency continues to increase, the motion of the wave energy converter becomes periodic in sinusoidal form again (Fig.13(c)~(d)).

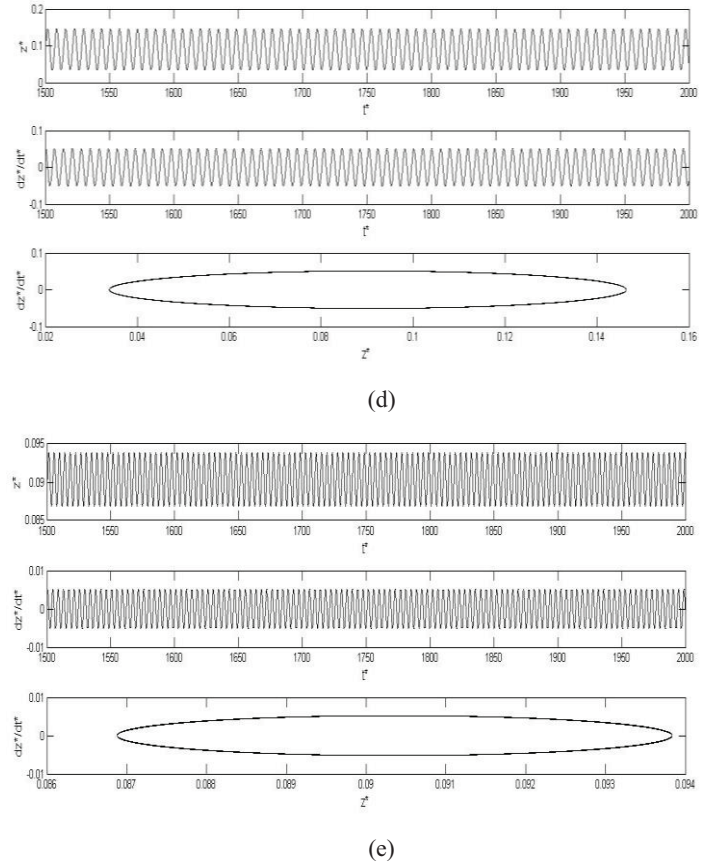
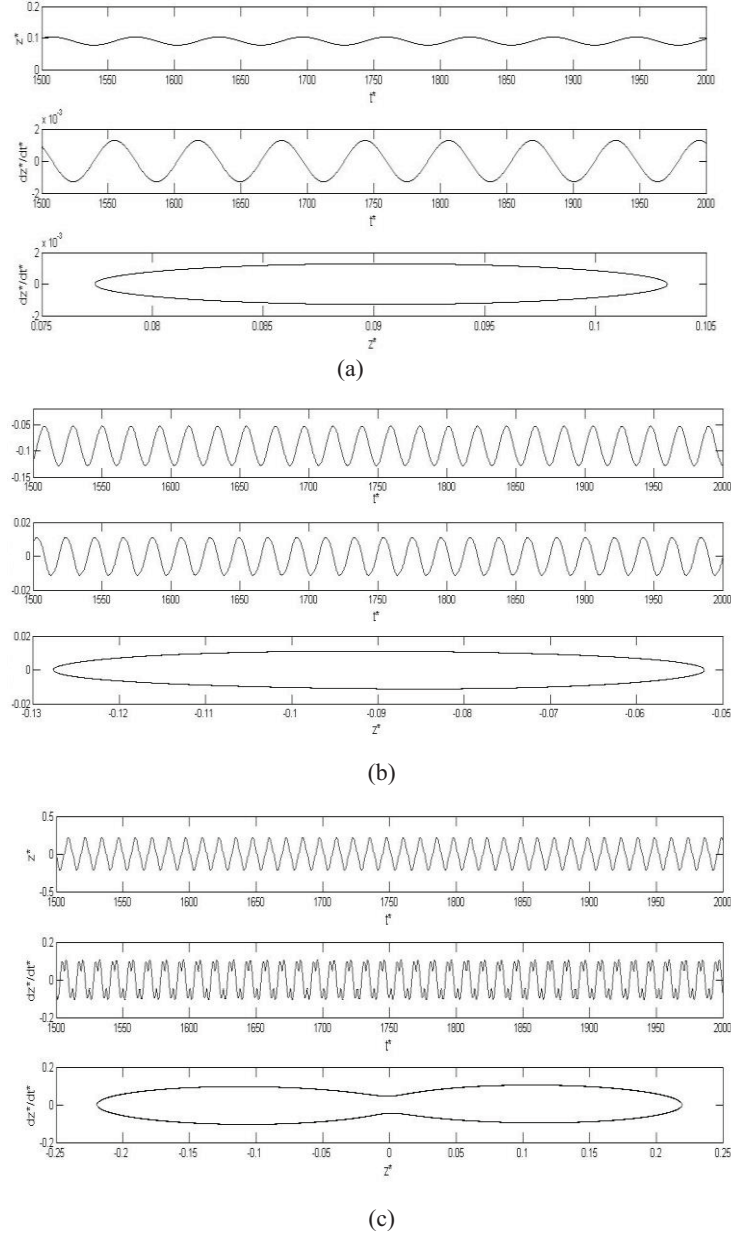
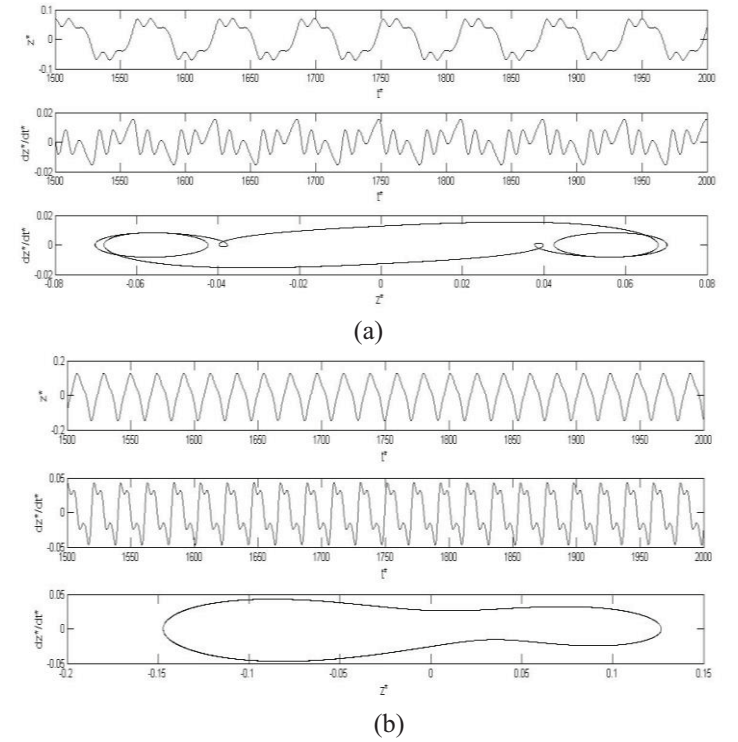
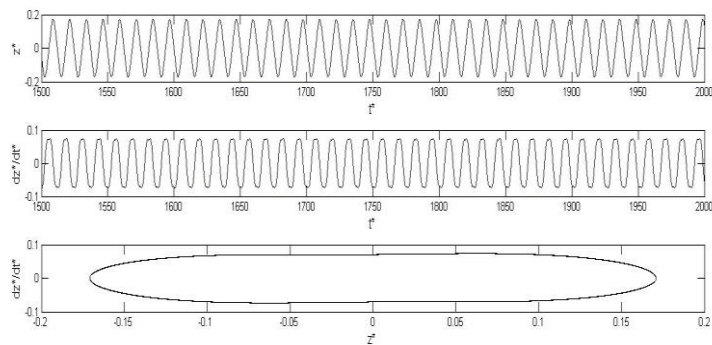
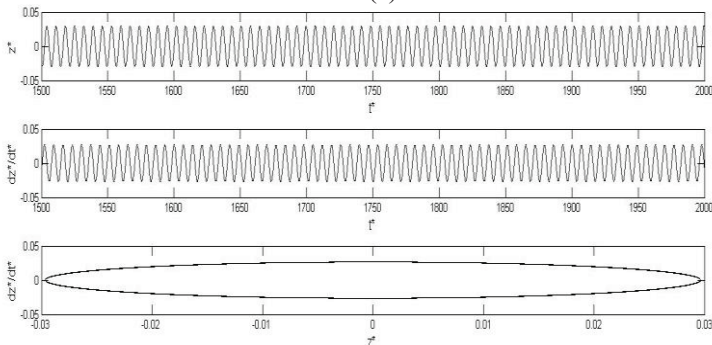


Fig.12 Steady state time history of the displacement and velocity response and the phase portraits for $A_{\omega}^* = 0.1$, $C^* = 0.3$, $\gamma = 0.01$, $K^* = 0.1$: (a) $\omega^* = 0.1$, (b) $\omega^* = 0.3$, (c) $\omega^* = 0.5$, (d) $\omega^* = 0.9$, (e) $\omega^* = 1.5$

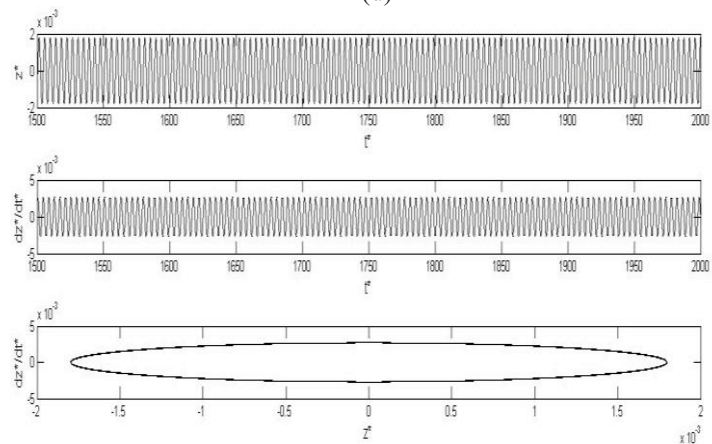




(c)



(d)



(e)

CONCLUSIONS

The work focuses on the response of linear and nonlinear converters in regular waves and analysis of the influence of several parameters on the power capture of linear and nonlinear converters. And comparisons are also made between the two types of PTO systems.

First the static characteristic of the nonlinear snap through mechanism with two symmetrically oblique springs is analyzed in detail. The snap through mechanism is characteristic of negative stiffness and double-well potential.

Then the response of linear and nonlinear converters in regular waves for a series of frequencies is numerically solved. The motion of the converter with nonlinear snap through PTO mechanism may be periodic or chaotic in terms of the amplitude and frequency of regular waves. The averaged power absorbed by the nonlinear PTO systems is greatly larger than that by linear systems at relatively low frequency input, while less than linear converters nearby resonance frequency or at high

frequency input. The difference of absorbed power between linear and nonlinear converters decreases with input amplitude becoming larger. An increase in damping coefficient near the optimum value of resonance frequency generates more energy harvested by linear and nonlinear converters.

ACKNOWLEDGEMENTS

The project is supported by the Independent Research Project of State Key Laboratory of Ocean Engineering in Shanghai Jiao Tong University (Grant No. GKZD010023).

REFERENCES

- Falcao, A.F., de, O., (2010). "Wave energy utilization: a review of the technologies," *Renewable Sustainable Energy Rev*, Vol 14, pp 899-918.
- Falnes, J., (2002). *Ocean Waves and Oscillating Systems*, Cambridge University Press, Cambridge.
- Faltinsen, O.M., (1990). *Sea loads on ships and offshore structures*, Cambridge University Press, pp 30-41.
- Hame, R. L., Wang, K. W. (2013). "A review of the recent research on vibration energy harvesting via bistable systems," *Smart Materials and Structures*, Vol 22, pp 023001.
- Hulme, A. (1982). "The wave forces acting on a floating hemisphere undergoing forced periodic oscillations," *J. Fluid Mech.* Vol 121, pp 443-463
- Ramlan, R., Brennan, M.J., Mace, B.R., Kovacic, R., (2010). "Potential benefits of a nonlinear stiffness in an energy harvesting device.," *Nonlinear Dynamics*, Vol 59, pp 545-558.
- Stanton S C, McGehee C C, Mann B P. (2010). "Nonlinear dynamics for broadband energy harvesting: Investigation of a bistable piezoelectric inertial generator," *Physica D: Nonlinear Phenomena*, Vol 239, pp 640-653.
- Tang, L., Yang, Y., and Soh, C. K. (2010). "Toward broadband vibration-based energy harvesting," *Journal of Intelligent Material Systems and Structures*, Vol 21, pp1867-1897.
- Vicente, P. C., Falcão, A. F., & Justino, P. A. (2013). "Nonlinear dynamics of a tightly moored point-absorber wave energy converter," *Ocean Engineering*, Vol 59, pp 20-36.